Lymphology 43 (2010) 98-109

LYMPHATIC DRAINAGE OF THE SKULL BASE: COMPARATIVE ANATOMIC AND ADVANCED IMAGING STUDIES IN THE RABBIT AND HUMAN WITH IMPLICATIONS FOR SPREAD OF NASOPHARYNGEAL CARCINOMA

Z. Qiuhang, W. Zhenlin, Q. Yan, H. Jun, S. Yongfeng, H. Bo

Center of Skull Base Surgery, China INN and Department of Otolaryngology-Head and Neck Surgery (ZQ,WZ,QY,HJ), Xuanwu Hospital, Capital Medical University, Beijing; Department of Otolaryngology-Head and Neck Surgery (SY,HB), People's Hospital of Guangxi Zhuang Autonomous Region, Nanning, Peoples Republic of China

ABSTRACT

This preliminary study investigated the lymphatic drainage and distribution of lymphatic structures in the skull base. Characteristics of the rabbit skull base were analyzed and compared correspondingly with those of the human skull. The lymphatic circulation in the rabbit cranial base was detected by digital subtraction angiography (DSA), and lymph drainage in the human skull base was illustrated by interstitial magnetic resonance lymphography (MRL). Lymphatic structures and their distribution in MRL were identified by comparing with contrast-enhanced MRI and clinical data on basilar metastasis of nasopharyngeal carcinoma (NPC) in the human skull base. Anatomic similarity was found between the rabbit and human basilar regions. Well-visualized lymphatic pathways were found in the rabbit cranial base, and human lymphatic structures showed high signal intensity in enhanced T1-weighted MRL images. Lymphatic tissues in the human basilar region were found mainly distributed in the areas of the jugular foramen, foramen lacerum, and petrosal section of the internal carotid artery (ICA). Their distribution in the human basilar region was similar to the distribution in the rabbit basilar region and consistent with our clinical findings of the predilection sites of NPC metastasis in the skull base. Our studies show that bilateral symmetrical lymphatic structures were distributed along the ICA, internal jugular vein, and dura of cranial base in the central part of the middle and posterior skull base.

Keywords: comparative anatomy, lymphatic metastasis, lymphography, magnetic resonance imaging, nasopharyngeal cancer, skull base

Nasopharyngeal carcinoma (NPC) is the commonest epithelial cancer arising from the nasopharynx particularly in southern parts of China with an incidence rate of more than 2 per 100,000 (1,2). Metastases in the skull base are commonly seen in the terminal phases of NPC. In addition, when NPC spreads to skull base, the prognosis is poor. Due to recent improvement in neuro-imaging, the incidence of metastatic disease in the skull base and dura appears to be increasing. Most metastases to the cranial base are initially asymptomatic and may even be found serendipitously; further enlargement

often leads to progressive neurologic morbidity. Therefore, familiarity with metastatic pathways and frequent metastatic locations is necessary for detecting these lesions while they are still small, localized, and more responsive to treatment. Cancers can spread to the skull base via hematogenous spread from the primary tumor (3,4), by direct invasion along tissue spaces and muscles attached to skull base (5,6), or by lymphatic drainage. The former two metastatic pathways have been well documented by many anatomic and clinical studies. However, lymphatic drainage in the skull base has not been fully identified, and the pathways of lymphatic metastases remain to be elucidated.

During the past century, various tracers have been injected into the brain or subarachnoid space of several animal species to investigate clearance pathways. These materials have been found in cervical lymph nodes afterwards (7-9) providing evidence of lymphatic drainage pathways from the brain to the extracranial lymph system. Several recent case reports have also confirmed that some intracranial malignancies such as glioblastomas and gliomas metastasize to cervical lymph nodes (10,11). These studies also concluded that there is a lymphatic circulation draining lymph from the brain to the neck through the skull base. Moreover, lymph nodes invaded by malignant tumors have been found in the skull base area in a few reports, which supports that lymphatic tissues do exist in the skull base (12,13). Furthermore, in contrast to the basilar metastatic distribution along the clivus in other tumors, we found that metastatic lymph nodes in the skull base in NPC were distributed in a regular fashion, and most were located in the area between the foramen lacerum and jugular foramen (Zhang Qiuhang, MD, unpublished data). Based on the above evidence, we postulated that there is a lymph circulation in the skull base area connecting the brain to the neck and via this drainage pathway, intracranial tumors spread to extracranial lymph nodes, and systemic malignant tumors metastasize to the skull base. However, this lymph circulation in the skull base has not as yet been fully demonstrated. This study was designed to: examine characteristics of the rabbit skull base and compare these with the human skull to uncover the similarity in the bony structures; identify lymph circulation pathways in the basilar region of the rabbit using digital subtraction lymphography (DSL) (which suggests that a similar lymph system may exist in the skull base of humans); and depict the lymph drainage in the human skull base by interstitial magnetic resonance lymphography (interstitial MRL). The goal is to show important images of the local lymph circulation in the cranial base, provide clues to detect possible metastasic lesions in the basilar area, and improve the unsatisfactory five-year survival rate in patients with basilar malignancies.

SUBJECTS AND METHODS

The study was performed at two institutions (Xuanwu Hospital, Capital Medical University, Beijing, PR China, and People's Hospital of Guangxi Zhuang Autonomous Region, Nanning, PR China) according to sound clinical practice standards, with regulatory and institutional review board approval.

Animals

Forty healthy adult New Zealand white rabbits (each weighing 2.5-3.5kg) were obtained from the Animal Experiment Center of Capital Medical University. The experiment and procedure protocols conformed to the principles of laboratory animal care (NIH publication No.86-23, revised 1985) and approved by the Institutional Animal Care and Use Committee of Capital Medical University. Twenty (10 male, 10 female) rabbit skull specimens were obtained after sacrifice. In another twenty rabbits (10 male, 10 female), DSL was performed after

intubating their cervical lymphatic vessels under general anesthesia with intramuscular ketamine (50mg/kg; Pfizer, USA) and xylazine (10mg/kg; Bayer, Germany).

Subjects

Twenty-four patients with suspected nasopharyngeal carcinoma (14 men, 10 women; age range, 21-54 years; average 31.2 years) were equally and randomly assigned into two groups. Digital subtraction angiography (DSA) studies were conducted in one group, magnetic resonance (MR) and interstitial MRL examinations were performed in the other. The interval between the MR and interstitial MRL examinations was one week. Dynamic observation of contrast-enhanced phases was also performed in DSA, MR and interstitial MRL studies. Participants who were pregnant or lactating, had a history of allergy to gadopentetate dimeglumine or Omnipaque, or a history of surgery or vascular diseases in the head and neck were ineligible. The protocol was approved by the Institutional Review Boards and Ethics Committees of both institutions. Written informed consent was obtained from all subjects.

101 cases of NPC patients (admitted from September 2005 to March 2008; 83 males, 18 females; age range, 17-65 years; average 48.5 years) were reviewed retrospectively. The MR examination and pathological diagnosis in all cases were collected and studied regarding the distribution of lymphatic metastasis in the skull base.

Comparative Anatomic Observations in the Rabbit and Human Skull Bases

Twenty rabbits were euthanized with intracardiac pentobarbital (Sigma, USA). Skulls were harvested and all soft tissues were removed from the skulls by boiling, detaching, and rinsing so that a clear view of the fine bony structures was achieved. The skulls were then left to dry at room temperature before further observation. Twenty human skulls were provided by the Department of Anatomy at Capital Medical University. The following landmarks of all rabbit skull specimens were identified and compared with corresponding structures of the human: foramen magnum, foramen jugulare, foramen hypoglossi, foramen lacerum, apertura externa canalis carotici, anterior hiatus, foramen rotundum, foramen cavernous, and hypophysial fossa.

Digital Subtraction Lymphography (DSL) in Rabbits

DSL was performed by intubation of the right jugular lymphatic trunk of ten rabbits and the left jugular lymphatic trunk of the other ten as follows. The neck was turned to the opposite side of the incision in supine rabbits. The neck fur was clipped, and the skin was prepared with povidone iodine and 70% alcohol scrubs. A skin incision was made on the anterior border of the sternocleidomastoid muscle. The jugular lymphatic trunk with semitransparent thin wall was exposed lateral to the carotid sheath by blunt dissection of tissues under the microscope (Carl Zeiss, Germany). The proximal portion of the lymphatic trunk was temporarily blocked, and the trunk became dilated after gentle massage. A 5F microcatheter was introduced into the lymphatic trunk and distally ligated with the lymphatic trunk using 0 silk suture (Ethicon, USA). Proximal blockage was then released. Digital subtraction images were obtained during injection of 1-2 ml of nonionic contrast material (Omnipaque Sigma, USA) with a power injector (Bruker, Germany) at the rate of 0.1-0.2ml/min and pressure of 2kg/cm^3. DSL was performed with a digital subtraction angiographic unit (DSA unit; Siemens Axiom Artis, Siemens, Germany). Standard anteroposterior and lateral projections were routinely acquired.

MRI in the Human Skull Base Region

MR examinations were performed with a 3-T Siemens Trio system (Siemens, Germany) with an eight channel head coil. Contrast-enhanced MR angiography was performed after intravenous (ulnar vein) injection of 0.2mmol of Gadolinium Diethylenetriaminepentaacetic Acid (GD-DTPA, Bayer, Germany) per kilogram of body weight. Post-contrast images were obtained in axial and coronal using a 3-D Flash (Fast Low Angle Shot) sequence after injection. Imaging parameters were as follows: TR = 2.5ms, TE = 1.1ms, flip angle = 20°, matrix = 256 x 200, Fov = 300mm x 234mm, 144 slices, slice thickness = 1.2mm.

DSA in the Human Skull Base Region

DSA was performed transfemorally with 5F catheters using a bi-plane DSA unit (Siemens Axiom Artis, Siemens, Germany) with an image intensifier matrix of 1024(1024 pixels. DSA was performed with bilateral selective internal carotid artery (ICA) injections. Eight to ten milliliters of Omnipaque was used for each injection at a rate of 4-6 ml/sec using a power injector. Anteroposterior and lateral views were obtained.

Interstitial MRL in the Human Skull Base Region

A dose of 4.5 ml gadopentetate dimeglumine (GD, Bayer, Germany) and 0.5 ml of lidocaine 2% was subdivided into 5 portions, and each portion was endoscopically injected into one of bilateral submucosa of the pharyngeal recess. This water-soluble contrast agent was infused by a power injector (0.2 ml/min) using thin needles with a total amount of 1 ml per injection site. Directly after administration of the contrast material, the injection sites were massaged for approximately 60 seconds. MRI was repeated at 2, 8 and 35 minutes after application of the contrast agent. Axial and coronal T1 weighted images of the skull base were acquired. The interstitial MRL examinations of individual patients in the study were performed with a 1.5-T Siemens system (Siemens, Germany). The imaging parameters were: TR = 5.01ms, TE = 1.03ms, flip angle = 30°, matrix = 195 x 256, Fov = 300mm x 234mm, slice thickness = 1.3mm.

Image Analysis

Two independent radiologists (with 7 and 10 years of work experience, respectively) who were blinded to clinical history reviewed all DSA and MR studies. The images were presented in an anonymous random fashion. Each examination was allocated a study number known only to the study coordinator. Both readers were blinded to the assessments of the other technique or of the other investigator.

RESULTS

Comparative Anatomic Observation of the Rabbit and Human Skull Bases

Remarkable similarity in the bony structures of the skull base was found between rabbits and humans (*Fig. 1*). The rabbit skull base was roughly divided into four parts: the occipital region, acoustic region, sphenoidal region, and nasal capsule region. The occipital region was composed of supraoccipital bone, exoccipital bone, and basioccipital bone. The same structures such as foramen magnum, foramen jugulare, foramen hypoglossi, foramen lacerum, and same nerves and vessels that passed these foramina were also observed in the occipital region of the rabbit cranial base compared with those of humans. The rabbit acoustic region was made up by the petrous mastoidal bone, tympanic bulla, and mastoid. The location of the apertura externa canalis carotici in the rabbit acoustic area was similar to that in the human skull base. The rabbit sphenoidal region consisted of basisphenoid bone, presphenoid bone, alisphenoid bone and orbitosphenoid bone. The anterior hiatus, foramen rotundum and

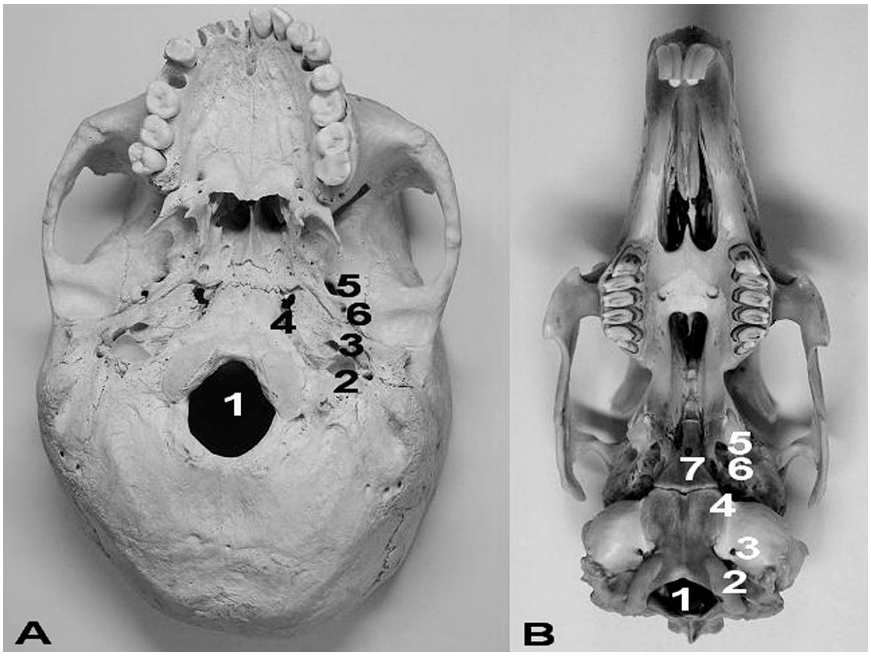

Fig. 1. Caudal view of mature rabbit and human skulls (A,B) display remarkable similarities in the bony structures of the skull base. Foramina in the human (A) and rabbit (B) skull bases are as follows: 1. foramen magnum, 2. jugular foramen, 3. apertura externa canalis carotici, 4. foramen lacerum, 5. foramen ovale, and 6. foramen spinosum. Also seen in the rabbit skull base in B is 7. foramen cavernous.

foramen ovale in the alisphenoid bone in the rabbit sphenoidal region corresponded to the superior orbital fissure, foramen rotundum and foramen ovale in the human basilar region. The same nerves in rabbits, such as the oculomotor nerve, ophthalmic nerve, maxillary nerve, and mandibular nerve, passed through these fissures and foramina as in humans. However, some differences were also found. There was a foramen cavernous in the center of the rabbit basisphenoid bone, which on ascending, led to the hypophyseal fossa, and a bigger optic foramen in the interorbital septum existed in the rabbit cranial base compared to the human basilar region. A madreporite, a perpendicular plate, and two ethmoidal labyrinths formed the rabbit nasal capsule region, and a similar multiporous perpendicular plate through which the olfactory nerve passed from nasal cavity to olfactory bulb in the brain was observed in the rabbit nasal capsule and in the human madreporite.

DSL in Rabbits

Distinct lymphatic structures including afferent and efferent lymphatic vessels, and lymph nodes were visualized in the rabbit basilar region in post-contrast images (*Fig. 2*). No differences were found in DSL image results between contrast injections through the left or right lymphatic trunks. Ascending flow of contrast agent from the neck to the skull base through lymphatic vessels was observed. The following basilar lymphatic structures appeared gradually: lymphatic ring and lymph node around the foramen magnum (*Fig. 2A,D*), then the lymphatic tissues near the jugular foramen, apertura externa canalis carotici and foramen lacerum (*Fig. 2B,E*), and lastly, the lymph node and lymphatic vessels near the foramen cavernous (*Fig. 2C,F*).

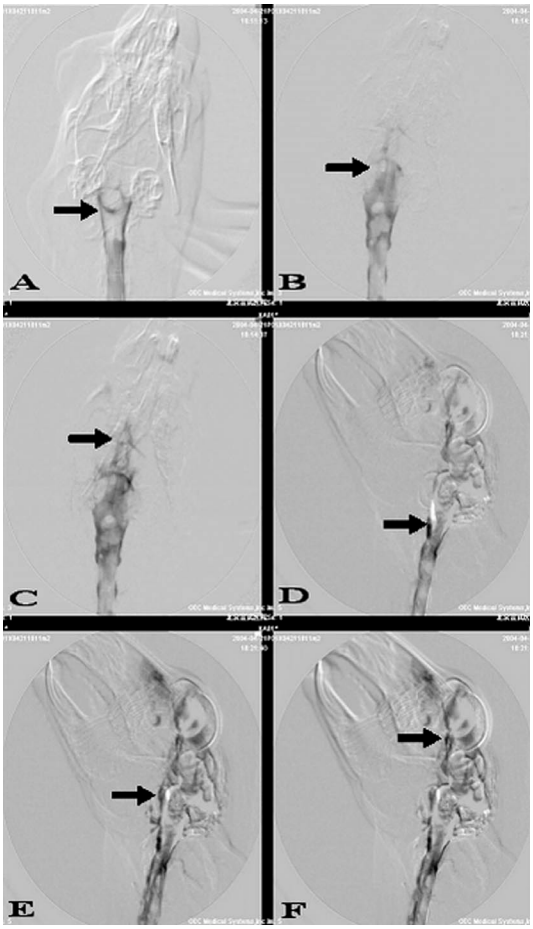

Fig. 2. Digital subtraction lymphography (DSL) in rabbit cranial base region displays the (A) Annular lymphatic structure near foramen magnum, skull posteroanterior (PA), (B) Annular lymphatic structure near jugular foramen and apertura externa canalis carotici, skull PA. (C) Triangulate lymphatic structure near cavernous foramen, skull PA, (D) Lymph node near foramen magnum, skull lateral (LAT), (E) Lymph node near jugular foramen and apertura externa canalis carotici, skull LAT, and (F) Lymph node near cavernous foramen, skull LAT.

Radiological Results in the Human Skull Base

All subjects completed the examinations successfully without significant adverse reaction to the contrast agents. The worst side effects of submucous contrast injection were brief with mild pain and swelling at the injected sites, which were self-limited. The technical quality of images was deemed sufficient in all subjects. Both on-site investigators and off-site blinded readers considered the technical quality of the images excellent with little or no difference in quality apparent between examinations.

The arteries and veins in the human skull base and brain were clearly visualized in DSA and MR post-contrast images without local enhancement around blood vessels. The arterial phase, capillary phase, and venous phase were observed after contrast agent injection in DSA examinations (*Fig. 3*). An obvious presence of Gd-labeled blood stream flowed from the neck to the intracalvarium through arteries and was cleared through veins on DSA. Enhanced arteries in the basilar region were detected at about 2 seconds after injection, and the contrast agent was completely cleared from the vessels 12 seconds after injection on DSA examinations. Arteries were clearly visualized about 5 seconds after injection (*Fig. 4A-D*), and venous phase appeared at approximately 35 seconds on MR examinations (*Fig. 4E-H*). The enhanced blood vessels were extensively distributed in the anterior, middle, and posterior basilar region both in DSA and MR postcontrast images.

In all MRL examinations, both of the bilateral lymphatics showed high signal intensity in T1-weighted images (*Fig. 5*). The lymphatic vessels extending from the injection site to skull base were clearly visualized at 2 minutes after injection (*Fig. 5G*), and the best delineation of the basilar lymphatic vessels was shown at 8 minutes (*Fig. 5A-F*). There was no obvious attenuation of intense signal at 35 minutes (*Fig. 5H*). Enhanced lymphatic vessels were observed along the ICA, internal jugular vein, and dura of the cranial base. The intense signals of lymphatic vessels were distributed from the posterior margin of the medial and lateral pterygoid to the clivus (*Fig. 5D-F*), and the lateral margin of the lymphatic signals reached the medialis border of the parotid

Fig. 3. Digital subtraction angiography (DSA) images of cranial base region of the human display dye in blood vessels in the basilar area and brain. The branches of ICA and internal jugular vein were distributed in the anterior, middle and posterior regions of the skull base and brain. Arterial phase (A), capillary phase (B) and venous phase (C) were identified in lateral DSA images.

gland. Symmetrical lymphatic structures were observed in the left and right sides of the basilar region, and the anastomosis of the bilateral lymphatic vessels was detected in the central skull base, which was anterior to the clivus (*Fig. 5C,F*). There were no apparent enhanced signals in the major blood vessels and intracalvarium at 2 and 8 minutes. Mild enhanced signals were found to appear in the extracranial internal jugular vein at 35 minutes as the contrast agent was transferred to the veins with reflux of lymph (*Fig. 5H*).

Basilar Lymphatic Metastasis in NPC Patients

In 101 cases of NPC patients, 17 cases were found to present lymphatic metastases in the skull base, which were confirmed by pathologic examination. The incidence of basilar lymphatic metastasis was 16.83%. Metastatic lesions were located in the region between apertura externa canalis carotici and foramen lacerum in 5 cases, in the jugular foramen region in 11 cases, and in the sella base in 1 case.

DISCUSSION

Metastatic lymph nodes in the human skull base have been found in malignant tumors such as NPC in some studies (12,14), and malignancies with basilar lymphatic metastasis have a poor prognosis. To improve the unsatisfactory control of these tumors, identification of the lymphatic drainage pathways is necessary. Moreover, assessment of the regional lymphatic system in the basilar region offers clinically important information for determination of prognosis, earlier discovery of metastatic lesions, and treatment planning including radical resection of the primary tumor and metastatic lymph nodes in the skull base. While most previous studies on lymphatic drainage have focused on the lymphatic tissues of limbs, neck, and trunk (15-17), the lymphatic pathways in the skull base have been largely unknown. Our present research provides a clue to the human basilar lymphatic circulation from a comparative anatomic study of the rabbit and human cranial bases. Furthermore, we delineated the lymphatic drainage in the human skull base by interstitial MRL.

In this research, a comparative study of the rabbit and human cranial bases formed the basis for further study of lymphatic structures in the human basilar area. Similar skull components, foramina, homonymous blood vessels and nerves were found in the cranial base of both rabbits and humans. Moreover, distinct lymphatic vessels and nodes were detected in the rabbit skull base

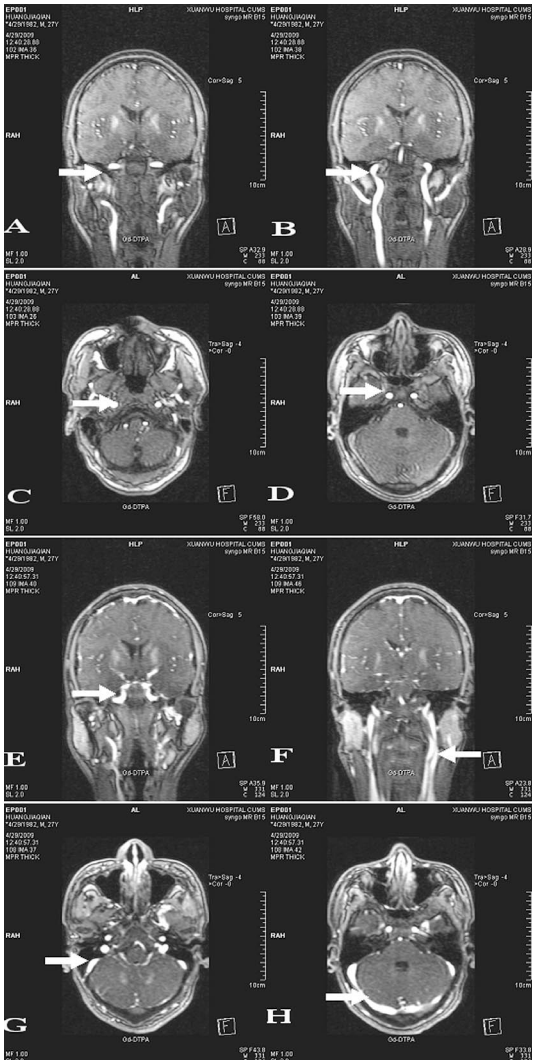

Fig. 4. Contrast-enhanced magnetic resonance (MR) images of the human cranial base region. Clear arterial phase (A-D) and venous phase (E-H) were observed in T1-weighted MR images after contrast agent injection. The arteries and veins in the human skull base and brain were well visualized on MR images without local enhancement out of blood vessels. Arrows point to the following: (A) Internal carotid canal segment of ICA, head coronal view, (B) Transition location of ICA from cervical segment to internal carotid canal segment, head coronal view, (C) Cervical segment of ICA, head axial view, (D) Cavernous sinus segment of ICA, head axial view, (E) Cavernous sinus, head coronal view, (F) Cervical segment of internal jugular vein located on the lateral margin of ICA, head coronal view, (G) G: Sigmoid sinus, head axial view, and (H) Transverse sinus, head axial view.

by DSL, and these lymphatic tissues were located near the foramina and hiatus through which blood vessels and nerves passed in the skull base. Further, metastatic lymph nodes have been found near these blood vessels and nerves in the human skull base in previous studies and our own clinical work on NPC treatment (18,19). According to these findings, we postulated that there were similar lymphatic drainage pathways in the human and rabbit basilar region.

To demonstrate the lymphatic circulation in the human skull base, satisfactory lymphography had to be obtained. The invasiveness and ethical restrictions of direct lymphangiography in humans as well as the poor morphologic imaging resolution of lymphoscintigraphy mitigated against the use of these imaging methods. MRI has potential clinical applications in detection of lymphatic structures in patients with lymphatic metastasis and disorders of lymphatic circulation (20,21). Gd-enhanced T1-weighted MR images provide a higher spatial resolution, higher signal to noise ratio, and fewer artifacts than T2-weighted images. Recently, interstitial T1-weighted MRL with water-soluble, Gd-based contrast agents has been shown to be safe, feasible and reliable in displaying the lymphatic structures in peripheral lymphedema and for sentinel node detection in systemic carcinomas (22,23). Due to the lack of radiation, MRL shows great promise in repeatable, accurate and optimized lymphatic visualization in lymphatic disorders. However, a safe and effective method of interstitial MRL had not been developed for studies on the human basilar lymphatic circulation. In this study, local swelling and pain were minor after the submucosal injection of contrast agent in MRL examinations. We suspect that the minimal side effects may relate to the small volume of injection and the analgesic effect of lidocaine. Our experience is consistent with previous findings that submucosal interstitial MRL with GD is safe for humans (24,25).

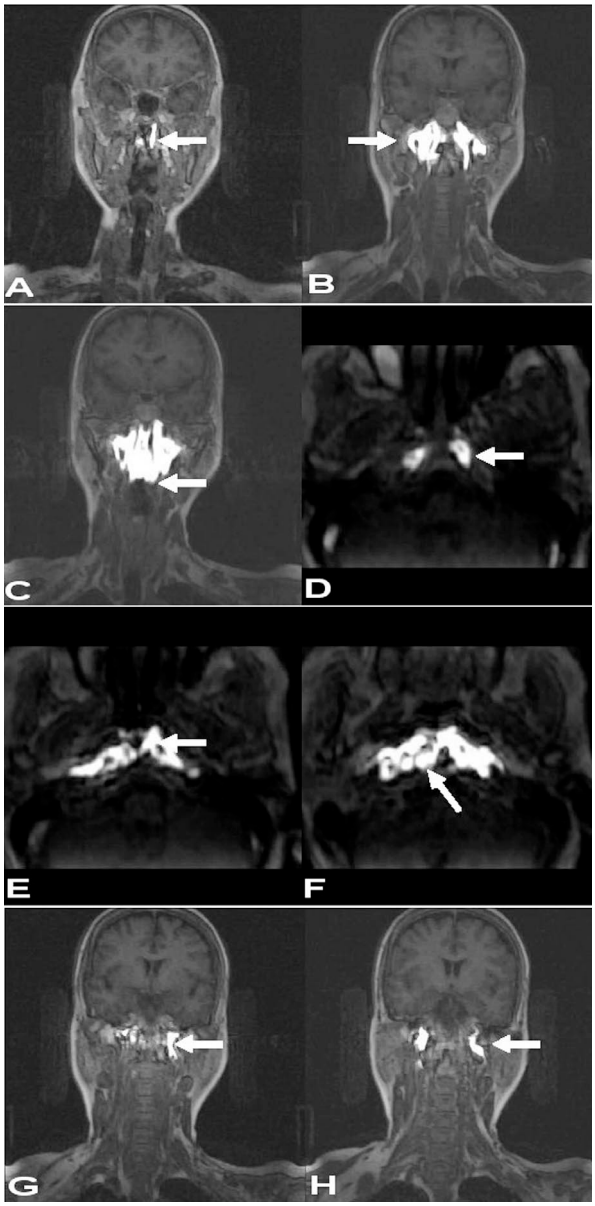

Fig. 5. Interstitial magnetic resonance lymphography (interstitial MRL) images of the human cranial base region 8 minutes after contrast agent injection (A-F). Bilateral symmetrical lymphatic structures show high signal intensity in T1-weighted MRL images. Enhanced signals in lymphatic vessels showed apparent ascending directionality from the injection site to skull base (A, arrow) and enhanced lymphatic vessels were observed along ICA, internal jugular vein, and dura of cranial base (B-H, arrows). The basilar lymphatic structures were distributed in the central part of the middle and posterior skull base (A-H) and anastomosis of bilateral lymphatic vessels was detected in the central skull base anterior to clivus (C,F). A suspicious lymph node was found in the skull base in MRL images (F, arrow). No apparent enhanced signals in the major blood vessels and intracalvarium were observed in MRL images at 2 (G) and 8 minutes (A-F) after contrast injection, and enhanced vein signals were found at 35 minutes (H). The circumvascular lymphatic vessels displayed intensively enhanced signal in the middle segment, and mildly enhanced signal in the superior and inferior segments presented signal caused by refluxed contrast in the extracranial internal jugular vein (H, arrow).

The high-resolution T1-weighted MRL protocol described herein allowed differentiation between lymphatic vessels and blood vessels in the basilar region by comparison with contrast-enhanced MR and DSA. The lymphatic drainage pathways were sufficiently and selectively enhanced against the background tissues in MRL images. Regular circumvascular distribution of enhanced signals of GD in MRL images indicated that contrast agent was absorbed through lymphatic vessels rather than blood vessels. Blood vessels were also distinguished from lymphatic vessels by flow empty phenomena in the same MRL images. In addition, the enhanced lymphatic vessels were mainly distributed in the middle and posterior parts of the skull base between the bilateral infratemporal fossa without enhanced signals in the intracalvarium on MRL images. However, widespread existence of blood vessels in the whole basilar area and inside the brain was observed on intravenous enhanced MR and DSA images. Another difference also helped to distinguish enhanced lymphatic vessels from blood vessels. There was an apparent arterial phase and venous phase in contrast-enhanced MR and DSA. Because contrast agent was rapidly washed out by the bloodstream, the enhanced signals in blood vessels attenuated quickly. However, the enhanced lymphatic vessels persisted much longer and without phase alteration. Another question yet to be answered is whether proactive lymphatic absorption and/or free diffusion along interstitial space are possible mechanisms by which the contrast agent was transferred from the injection site to skull base. In MRL images, enhanced signals in lymphatic vessels showed apparent ascending directionality from the injection site to the skull base, which was different from the uncontrolled diffusion along tissue spaces from the injection sites. The appearance of contrast agent in the lymph vessels in 2 minutes suggests that it was not a passive diffusion along the tissue space but a rapid active agent uptake from the nasopharyngeal injection sites through the lymphatic circulation. Besides, some consistent findings in basilar lymphatic distribution between rabbits and humans were identified by comparison of MRL in humans and DSL in rabbits in this study. The basilar lymphatic structures were distributed in the central part of the middle and posterior skull base and located around the major blood vessels, which was also consistent with the distribution of lymphatic structures in the neck. These results all confirm our hypothesis that bilateral lymphatic drainage pathways exist in the human basilar region.

In the present study, the lymphatic tissue appears to be a plaque-like enhancement, and afferent and efferent lymphatic vessels were not clearly distinguished on MRL images. We speculate that this was due to opacification of congested tiny peripheral lymphatic vessels. Although suspicious lymph nodes were observed on MRL images, definite nodes were not identified with certainty. We suspect that lymph nodes could be masked by the artifacts of intensive plaquelike enhanced signal of lymphatic tissue. Similarly, as mentioned in prior MRL studies with extracellular water-soluble, micromolecular contrast agents, lymph node enhancement was not sufficient for identification of nodal morphology (26,27).

Although the exact mechanism of GD uptake by lymphatics is unknown, it probably drained from the interstitial space to the lymphatic pathways through the thin-walled and fenestrated lymphatic capillary, which may depend on a combined effect of pressure, osmosis, and volumes (28,29). The submucosal injection in interstitial MRL may facilitate migration of contrast agent into lymphatics due to the effect of high pressure in connective tissues. Moreover, massage of the injection sites also enhanced lymphatic transfer of the contrast agent.

In this study, the reason for selecting the pharyngeal recess as the injection site in MRL was that this is the most frequent site of NPC. Moreover, familiarity with the

lymphatic circulation from the pharyngeal recess to the skull base may help in earlier detection of NPC basilar metastases justifying a radical treatment plan. In addition, the location of lymphatic structures in the human basilar region was found distributed mainly in the areas of the jugular foramen, foramen lacerum, and petrosal section of ICA on MRL images, which was consistent with our clinical findings of predilection sites for NPC metastasis in the skull base.

Although we delineated the lymphatic circulation in the human skull base by interstitial MRL, there were several limitations in this research. The range of the visualized lymphatic pathways may have been affected by the location of the injection sites, and the delivery of the contrast agent was only limited to local nodes. Therefore, multiple interstitial injections may be necessary to cover the whole suspected area. In the present study, we selected the pharyngeal recess as the injection site, and the detected lymphatic circulation may represent the pathways from the nasal pharynx to the skull base. Selection of multiple injection sites would be helpful to obtain more details and a comprehensive picture of the lymphatic circulation in the human basilar region. Furthermore, because gadopentetate dimeglumine is a low-molecular contrast agent, possibly contaminated veins may be confused with lymphatic vessels and cannot be thoroughly avoided in interstitial MRL. Application of macromolecular agents that can only be cleared through lymphatic vessels would eliminate this interference. We also attempted retrograde injection of contrast agent into the human jugular lymphatic trunk to observe the lymphatic circulation in the skull base by DSA in several neck dissection operations. Contrast agent was found to leak into the tissue space of the neck shortly after injection no matter how the injection pressure was adjusted. This failure to fill human basilar lymphatics from the jugular lymphatic trunk may relate to the fragile wall of the thinner human lymphatic vessels compared to the rabbit.

CONCLUSION

In summary, our study clearly demonstrates that there are anatomic similarities between the rabbit and human basilar regions and that definite lymphatic pathways were detected in the rabbit cranial base. Furthermore, the lymphatic circulation in the human basilar region was observed and distinguished from blood vessels by contrast-enhanced MR and interstitial MRL. MRL provided a safe, objective diagnostic method and sufficient follow-up information in patients with basilar metastases. Our findings also provide a deeper insight into the human basilar lymphatic system and clues to targeting the lymphatic circulation as a more precise strategy for earlier diagnosis and better control of metastases in the skull base.

ACKNOWLEDGMENTS

This work was supported by a research grant from the Capital Development Foundation of China (2005-1035).

REFERENCES

1. Ng, WT, CW Choi, MC Lee, et al: Familial nasopharyngeal carcinoma in Hong Kong: epidemiology and implication in screening. Fam. Cancer 8 (2009), 103-108.
2. Cao, KJ, QY Fan, YL Liu, et al: Cancer incidence and mortality in Guangzhou City from 2000 to 2002. Ai Zheng 27 (2008), 225-230.
3. Cheng, SH, SY Tsai, KL Yen, et al: Prognostic significance of parapharyngeal space venous plexus and marrow involvement: potential landmarks of dissemination for stage I-III nasopharyngeal carcinoma. Int. J. Radiat. Oncol. Biol. Phys. 61 (2005), 456-465.
4. Feiz-Erfan, I, G Rao, WL White, et al: Efficacy of trans-septal trans-sphenoidal surgery in correcting visual symptoms caused by hematogenous metastases to the sella and pituitary gland. Skull Base 18 (2008), 77-84.
5. Lee, CC, ST Chu, P Chou, et al: The prognostic influence of prevertebral space involvement in nasopharyngeal carcinoma. Clin. Otolaryngol. 33 (2008), 442-449.

6. Wei, Y, J Xiao, L Zou: Masticator space: CT and MRI of secondary tumor spread. Am. J. Roentgenol. 189 (2007), 488-497.
7. Koh, L, G Nagra, M Johnston: Properties of the lymphatic cerebrospinal fluid transport system in the rat: Impact of elevated intracranial pressure. J. Vasc. Res. 44 (2007), 423-432.
8. Walter, BA, VA Valera, S Takahashi, et al: Evidence of antibody production in the rat cervical lymph nodes after antigen administration into the cerebrospinal fluid. Arch. Histol. Cytol. 69 (2006), 37-47.
9. Weller, RO, E Djuanda, HY Yow, et al: Lymphatic drainage of the brain and the pathophysiology of neurological disease. Acta Neuropathol. 117 (2009), 1-14.
10. Matalka, I, M Alorjani, F Kanaan, et al: Medulloblastoma in an adult with cervical lymph node metastasis: A case report and review of the literature. Pathology 41 (2009), 197-199.
11. Volavsek, M, J Lamovec, M Popovi: Extraneural metastases of anaplastic oligodendroglial tumors. Pathol. Res. Pract. 205 (2009), 502-507.
12. Chen, SM, CN Chang, KC Wei, et al: Sellar lymphoma mimicking sphenoid infection presenting with cavernous sinus syndrome. J. Clin. Neurosci. 15 (2008), 1148-1151.
13. Choi, HK, JE Cheon, IO Kim, et al: Central skull base lymphoma in children: MR and CT features. Pediatr. Radiol. 38 (2008), 863-867.
14. Olajos, J, E Füle, J Erfán, et al: Familial clustering of nasopharyngeal carcinoma in a non-endemic geographical region. Report of two Hungarian cases and a review of the literature. Acta Otolaryngol. 125 (2005), 1008-1013.
15. Moseley, AL, CJ Carati, NB Piller: A systematic review of common conservative therapies for arm lymphoedema secondary to breast cancer treatment. Ann. Oncol. 18 (2007), 639-646.
16. Uren, RF, RB Howman-Giles, D Chung, et al: Role of lymphoscintigraphy for selective sentinel lymphadenectomy. Cancer Treat. Res. 127 (2005), 15-38.
17. van der Ploeg, IM, RA Valdés Olmos, BB Kroon, et al: The yield of SPECT/CT for anatomical lymphatic mapping in patients with melanoma. Ann. Surg. Oncol. 16 (2009), 1537-1542.
18. Dubrulle, F, R Souillard, R Hermans: Extension patterns of nasopharyngeal carcinoma. Eur. Radiol. 17 (2007), 2622-2630.
19. Laigle-Donadey, F, S Taillibert, N Martin-Duverneuil, et al: Skull-base metastases. J. Neurooncol. 75 (2005), 63-69.
20. Lohrmann, C, E Foeldi, M Langer: MR imaging of the lymphatic system in patients with lipedema and lipo-lymphedema. Microvasc. Res. 77 (2009), 335-339.
21. Narayanan, P, T Iyngkaran, SA Sohaib, et al: Magnetic resonance lymphography: A novel technique for lymph node assessment in gynecologic malignancies. Cancer Biomark 5 (2009), 81-88.
22. Clément, O, A Luciani: Imaging the lymphatic system: Possibilities and clinical applications. Eur. Radiol. 14 (2004), 1498-1507.
23. Lohrmann, C, E Foeldi, JP Bartholomä, et al: Interstitial MR lymphangiography - a diagnostic imaging method for the evaluation of patients with clinically advanced stages of lymphedema. Acta Trop. 104 (2007), 8-15.
24. Dimakakos, E, A Koureas, V Koutoulidis, et al: Interstitial magnetic resonance lymphography: The clinical effectiveness of a new method. Lymphology 41 (2008), 116-125.
25. Loo, BW Jr, MT Draney, R Sivanandan, et al: Indirect MR lymphangiography of the head and neck using conventional gadolinium contrast: A pilot study in humans. Int. J. Radiat. Oncol. Biol. Phys. 66 (2006), 462-468.
26. Lohrmann, C, E Foeldi, O Speck, et al: High-resolution MR lymphangiography in patients with primary and secondary lymphedema. Am. J. Roentgenol. 187 (2006), 556-561.
27. Ruehm, SG, T Schroeder, JF Debatin: Interstitial MR lymphography with gadoterate meglumine: Initial experience in humans. Radiology 220 (2001), 816-821.
28. Misselwitz, B, H Schmitt-Willich, M Michaelis, et al: Interstitial magnetic resonance lymphography using a polymeric t1 contrast agent: Initial experience with Gadomer-17. Invest. Radiol. 37 (2002), 146-151.
29. Staatz, G, CC Nolte-Ernsting, GB Adam, et al: Interstitial T1-weighted MR lymphography: Lipophilic perfluorinated gadolinium chelates in pigs. Radiology 220 (2001), 129-134.

Zhang Qiuhang, MD, PHD
Center of Skull Base Surgery, China INN
Department of Otolaryngology-
Head and Neck Surgery
Xuanwu Hospital
Capital Medical University
Beijing 100053, PR China
Telephone: 0086-10-8319-8446
Fax: 0086-10-8319-8851
Email: shengxuewuyan@hotmail.com